

Supporting information for

$(\eta^3\text{-Allyl})\text{Ni(II)}$, Pd(II) , and Pt(II) Complexes Bearing a Bidentate Titanium(IV) Phosphinoamide Ligand: a $\text{Ti} \leftarrow \text{M}$ Dative Bond Enhances the Electrophilicity of the $\pi\text{-Allyl}$ Moiety

Hironori Tsutsumi,[‡] Yusuke Sunada,[†] Yoshihito Shiota,[†] Kazunari Yoshizawa,[†]

and Hideo Nagashima^{†,‡,*}

[†]Institute for Materials Chemistry and Engineering, and [‡]Graduate School of Engineering Sciences,

* Corresponding author. E-Mail: nagasima@cm.kyushu-u.ac.jp

[†] Institute for Materials Chemistry and Engineering, Kyushu University.

[‡] Graduate School of Engineering Sciences, Kyushu University.

Contents

Experimental Procedure

Figure S1. ^1H , ^{13}C , ^{19}F , and ^{31}P NMR spectra of $[(\eta^3\text{-methallyl})\text{Ni}(\text{Ph}_2\text{PN}^t\text{Bu})_2\text{TiCl}_2](\text{OTf})$ (**2a**)

Figure S2. ^1H , ^{13}C , ^{19}F , and ^{31}P NMR spectra of $[(\eta^3\text{-methallyl})\text{Pd}(\text{Ph}_2\text{PN}^t\text{Bu})_2\text{TiCl}_2](\text{OTf})$ (**2b**)

Figure S3. ^1H and ^{31}P NMR spectra of $[(\eta^3\text{-methallyl})\text{Pt}(\text{Ph}_2\text{PN}^t\text{Bu})_2\text{TiCl}_2](\text{OTf})$ (**2c**)

Figure S4. VT- ^1H and ^{31}P NMR spectra of $[(\eta^3\text{-methallyl})\text{Ni}(\text{Ph}_2\text{PN}^t\text{Bu})_2\text{TiCl}_2](\text{OTf})$ (**2a**)

Figure S5. VT- ^1H and ^{31}P NMR spectra of $[(\eta^3\text{-methallyl})\text{Pd}(\text{Ph}_2\text{PN}^t\text{Bu})_2\text{TiCl}_2](\text{OTf})$ (**2b**)

Figure S6. ESI-(tof)-MS spectrum of $[(\eta^3\text{-methallyl})\text{Ni}(\text{Ph}_2\text{PN}^t\text{Bu})_2\text{TiCl}_2](\text{OTf})$ (**2a**)

Figure S7. ESI-(tof)-MS spectrum of $[(\eta^3\text{-methallyl})\text{Pd}(\text{Ph}_2\text{PN}^t\text{Bu})_2\text{TiCl}_2](\text{OTf})$ (**2b**)

Figure S8. ESI-(tof)-MS spectrum of $[(\eta^3\text{-methallyl})\text{Pt}(\text{Ph}_2\text{PN}^t\text{Bu})_2\text{TiCl}_2](\text{OTf})$ (**2c**)

Table S1. Crystallographic data for **2a**, **2b**, and **2c**.

Table S2. Representative bond lengths and angles for **2a**, **2b**, and **2c**.

Figure S9. ORTEP representation of the molecular structure of $[(\eta^3\text{-methallyl})\text{Ni}(\text{Ph}_2\text{PN}^t\text{Bu})_2\text{TiCl}_2](\text{OTf})$ (**2a**)

Figure S10. Gaussview depiction of HOMO for the calculated complex $[(\eta^3\text{-methallyl})\text{Ni}(\text{Ph}_2\text{PN}^t\text{Bu})_2\text{TiCl}_2](\text{OTf})$ (**2a**)

Figure S11. ORTEP representation of the molecular structure of $[(\eta^3\text{-methallyl})\text{Pd}(\text{Ph}_2\text{PN}^t\text{Bu})_2\text{TiCl}_2](\text{OTf})$ (**2b**)

Figure S12. Gaussview depiction of HOMO-1 for the calculated complex $[(\eta^3\text{-methallyl})\text{Pd}(\text{Ph}_2\text{PN}^t\text{Bu})_2\text{TiCl}_2](\text{OTf})$ (**2b**)

Figure S13. ORTEP representation of the molecular structure of $[(\eta^3\text{-methallyl})\text{Pt}(\text{Ph}_2\text{PN}^t\text{Bu})_2\text{TiCl}_2](\text{OTf})$ (**2c**)

Figure S14. Gaussview depiction of HOMO for the calculated complex $[(\eta^3\text{-methallyl})\text{Pt}(\text{Ph}_2\text{PN}^t\text{Bu})_2\text{TiCl}_2](\text{OTf})$ (**2c**)

Experimental Procedure

General. Manipulation of air and moisture sensitive organometallic compounds was carried out under a dry argon atmosphere using standard Schlenk tube techniques associated with a high-vacuum line. All solvents were distilled over appropriate drying reagents prior to use (THF, hexane; $\text{Ph}_2\text{CO}/\text{Na}$, CH_2Cl_2 ; CaH_2 , acetone; MS 4A). ^1H , ^{13}C , ^{19}F , ^{31}P NMR spectra was recorded on a JEOL Lambda 600 or a Lambda 400 spectrometer at ambient temperature unless otherwise noted. ^1H , ^{13}C , and ^{31}P NMR chemical shifts (δ values) were given in ppm relative to the solvent signal (^1H , ^{13}C) or standard resonances (^{19}F ; external CF_3COOH , ^{31}P ; external 85% H_3PO_4). ESI mass spectra were recorded on a JEOL JMS-T100CS apparatus. Melting points were measured on a Yanaco SMP3 micro melting point apparatus. Elemental analyses were performed by a Perkin Elmer 2400II/CHN analyzer. Starting materials, titanium phosphinoamide ¹), $[(\eta^3\text{-methallyl})\text{NiCl}]_2$ ²), $[(\eta^3\text{-methallyl})\text{PdCl}]_2$ ³), $[(\eta^3\text{-methallyl})\text{PtCl}]_2$ ⁴) were synthesized by the method reported in the literature.

Preparation of $[(\eta^3\text{-methallyl})\text{Ni}(\text{Ph}_2\text{PN}^t\text{Bu})_2\text{TiCl}_2](\text{OTf})$ (2a**).** In a glove box, $[(\eta^3\text{-methallyl})\text{NiCl}]_2$ (70.3 mg, 0.24 mmol) and acetone (350 μL , 4.8 mmol) was mixed in CH_2Cl_2 (5 mL), and AgOTf (122 mg, 0.48 mmol) was added to this solution. The mixture was stirred at room temperature for 10 min, then CH_2Cl_2 solution (5 mL) of titanium phosphinoamide $(\text{Ph}_2\text{PN}^t\text{Bu})_2\text{TiCl}_2$ (**1**) (300 mg, 0.48 mmol) was added dropwise to this solution. The resulting mixture was stirred at room temperature for 30 min during which time the color of the solution changed from orange to dark red. The solvent was evaporated and the residue extracted with CH_2Cl_2 . The insoluble materials were filtered off through a pad of Celite, and the resulting filtrate was collected. Removal of volatiles followed by washing with hexane gave desired heterobimetallic complex (**2a**) as a red powder (242 mg, 57 %). Single crystals of **2a** were grown from CH_2Cl_2 /pentane. M.p.: 112 $^\circ\text{C}$. ^1H NMR (CD_2Cl_2 , r.t.) δ 1.41 (s, 3H, $(\text{CH}_2)_2\text{C}(\text{CH}_3)$), 1.45 (s, 18H, ^tBu), 3.66 (br s, 4H, $(\text{CH}_2)_2\text{C}(\text{CH}_3)$), 7.23 – 7.25 (m, 4H, Ph), 7.26 – 7.30 (m, 4H, Ph), 7.47 – 7.49 (m, 2H, Ph), 7.53 – 7.57 (m, 4H, Ph), 7.60 – 7.62 (m, 2H, Ph), 7.92 – 7.94 (m, 4H, Ph). ^1H NMR (CD_2Cl_2 , -90 $^\circ\text{C}$) δ 1.25 (s, 3H, $(\text{CH}_2)_2\text{C}(\text{CH}_3)$), 1.31 (s, 18H, ^tBu), 3.74 (br s, 2H, $(\text{CH}_2)_2\text{C}(\text{CH}_3)$), 3.86 (br s, 2H, $(\text{CH}_2)_2\text{C}(\text{CH}_3)$), 7.12 – 7.14 (m, 4H, Ph), 7.19 – 7.23 (m, 4H, Ph), 7.38 –

7.41 (m, 2H, Ph), 7.55 – 7.59 (m, 4H, Ph), 7.60 – 7.62 (m, 2H, Ph), 8.31 – 8.37 (m, 4H, Ph). ^{13}C NMR (CD_2Cl_2) δ 27.9 (CH_3 -methallyl), 32.3 (s, CMe_3), 71.5 (br s, CMe_3), 81.60 (br s, $\text{CH}_2=\text{C}(\text{Me})$), 128.7, 129.9, 130.0, 132.4, 132.9, 133.0, 133.9, 134.5 (Ph), 139.2 (br s, $\text{CH}_2=\text{C}(\text{Me})$). ^{19}F $\{^1\text{H}\}$ NMR (CD_2Cl_2 , r.t.) δ -82.0 (s). ^{31}P $\{^1\text{H}\}$ NMR (CD_2Cl_2 , r.t.) δ 14.1 (br s). ^{31}P $\{^1\text{H}\}$ NMR (CD_2Cl_2 , -90 °C) δ 13.2 (br s). Anal. Calcd. for $\text{C}_{37}\text{H}_{45}\text{Cl}_2\text{N}_2\text{P}_2\text{O}_3\text{F}_3\text{STiNi}$: C, 49.70; H, 5.07; N, 3.13. Found: C, 49.52; H, 4.87; N, 2.98 %. Exact mass (ESI-TOF): Calcd. for $^{12}\text{C}_{36}^{1}\text{H}_{45}^{14}\text{N}_2^{31}\text{P}_2^{35}\text{Cl}_2^{48}\text{Ti}^{58}\text{Ni}_1$: 743.12680. Found: 743.12751.

Preparation of $[(\eta^3\text{-methallyl})\text{Pd}(\text{Ph}_2\text{PN}^t\text{Bu})_2\text{TiCl}_2](\text{OTf})$ (2b**).** In a glove box, $[(\eta^3\text{-methallyl})\text{PdCl}]_2$ (40.3 mg, 0.1 mmol) and acetone (151 μL , 2.0 mmol) was mixed in CH_2Cl_2 (5 mL), and AgOTf (52.7 mg, 0.2 mmol) was added to this solution. The mixture was stirred at room temperature for 10 min, then CH_2Cl_2 solution (5 mL) of titanium phosphinoamide $(\text{Ph}_2\text{PN}^t\text{Bu})_2\text{TiCl}_2$ (**1**) (130 mg, 0.2 mmol) was added dropwise to this solution. The resulting mixture was stirred at room temperature for 30 min during which time the color of the solution changed from orange to red. The solvent was evaporated and the residue extracted with CH_2Cl_2 . The insoluble materials were filtered off through a pad of Celite, and the resulting filtrate was collected. Removal of volatiles followed by washing with hexane gave desired heterobimetallic complex (**2b**) as a red powder (140 mg, 73 %). Single crystals of **2b** were grown from CH_2Cl_2 /pentane. M.p.: 131 °C. ^1H NMR (CD_2Cl_2 , r.t.) δ 1.50 (s, 18H, ^tBu), 1.52 (s, 3H, $(\text{CH}_2)_2\text{C}(\text{CH}_3)$), 3.76 (br s, 4H, $(\text{CH}_2)_2\text{C}(\text{CH}_3)$), 7.13 – 7.16 (m, 4H, Ph), 7.21 – 7.24 (m, 4H, Ph), 7.38 – 7.41 (m, 2H, Ph), 7.55 – 7.59 (m, 4H, Ph), 7.58 – 7.62 (m, 2H, Ph), 7.89 – 7.93 (m, 4H, Ph). ^1H NMR (CD_2Cl_2 , -90 °C) δ 1.40 (s, 18H, ^tBu), 1.42 (s, 3H, $(\text{CH}_2)_2\text{C}(\text{CH}_3)$), 3.70 (br s, 4H, $(\text{CH}_2)_2\text{C}(\text{CH}_3)$), 7.03 – 7.06 (m, 4H, Ph), 7.13 – 7.17 (m, 4H, Ph), 7.32 – 7.34 (m, 2H, Ph), 7.45 – 7.50 (m, 4H, Ph), 7.53 – 7.56 (m, 2H, Ph), 8.27 – 8.31 (m, 4H, Ph). ^{13}C NMR (CD_2Cl_2) δ 27.5 (CH_3 -methallyl), 33.8 (s, CMe_3), 72.1 (t, CMe_3 , $J_{\text{C-P}} = 5.8$ Hz), 83.0 (t, $\text{CH}_2=\text{C}(\text{Me})$, $J_{\text{C-P}} = 11.6$ Hz), 128.5, 129.3, 129.6, 129.7, 131.4, 132.0, 132.3, 132.8 (Ph), 141.1 (t, $\text{CH}_2=\text{C}(\text{Me})$, $J_{\text{C-P}} = 4.3$ Hz). ^{19}F $\{^1\text{H}\}$ NMR (CD_2Cl_2 , r.t.) δ -82.1 (s). ^{31}P $\{^1\text{H}\}$ NMR (CD_2Cl_2 , r.t.) δ 9.75 (s). ^{31}P $\{^1\text{H}\}$ NMR (CD_2Cl_2 , -90 °C) δ 8.56 (s). Anal. Calcd. for

C₃₇H₄₅Cl₂N₂P₂O₃F₃STiPd: C, 47.18; H, 4.82; N, 2.97. Found: C, 46.82; H, 4.54; N, 2.68 %. Exact mass (ESI-TOF): Calcd. for ¹²C₃₆¹H₄₅¹⁴N₂³¹P₂³⁵Cl₂⁴⁸Ti₁¹⁰⁶Pd₁: 791.09493. Found: 791.09391.

Preparation of [(η³-methallyl)Pt(Ph₂PN^tBu)₂TiCl₂](OTf) (2c). In a glove box, [(η³-methallyl)PtCl]₂ (45 mg, 0.08 mmol) and acetone (116 μL, 1.6 mmol) was mixed in CH₂Cl₂ (5 mL), and AgOTf (40.7 mg, 0.16 mmol) was added to this solution. The mixture was stirred at room temperature for 10 min, then CH₂Cl₂ solution (5 mL) of titanium phosphinoamide (Ph₂PN^tBu)₂TiCl₂ (**1**) (100 mg, 0.16 mmol) was added dropwise to this solution. The resulting mixture was stirred at room temperature for 30 min during which time the color of the solution changed from orange to dark red. The solvent was evaporated and the residue extracted with CH₂Cl₂. The insoluble materials were filtered off through a pad of Celite, and the resulting filtrate was collected. Removal of volatiles followed by washing with hexane gave desired heterobimetallic complex (**2c**) as a orange powder (128 mg, 81 %). Single crystals of **2c** were obtained by cooling the saturated toluene solution at - 35 °C. M.p.: 138 °C. ¹H NMR (CD₂Cl₂, r.t.) δ 1.51 (s, 18H, ^tBu), 1.76 (s, 3H, (CH₂)₂C(CH₃)), 3.46 (br s, 2H, (CH₂)₂C(CH₃)), 3.55 (br s, 2H, (CH₂)₂C(CH₃)), 7.12 – 7.15 (m, 4H, Ph), 7.18 – 7.22 (m, 4H, Ph), 7.34 – 7.37 (m, 2H, Ph), 7.44 – 7.46 (m, 4H, Ph), 7.53 – 7.57 (m, 2H, Ph), 7.80 – 7.84 (m, 4H, Ph). ¹H NMR (CD₂Cl₂, -90 °C) δ 1.40 (s, 18H, ^tBu), 1.68 (s, 3H, (CH₂)₂C(CH₃)), 3.70 (br s, 4H, (CH₂)₂C(CH₃)), 7.15 – 7.19 (m, 4H, Ph), 7.26 – 7.30 (m, 4H, Ph), 7.33 – 7.38 (m, 2H, Ph), 7.49 – 7.54 (m, 4H, Ph), 7.60 – 7.62 (m, 2H, Ph), 8.16 – 8.20 (m, 4H, Ph). The measurement of satisfactory ¹³C NMR spectrum was unsuccessful due to its poor solubility. ³¹P {¹H} NMR (CD₂Cl₂, r.t.) δ 0.60 (s with a satellite signal due to the coupling with ¹⁹⁵Pt, J_{Pt-P} = 3262 Hz). ³¹P {¹H} NMR (CD₂Cl₂, -90 °C) δ -0.16 (s with a satellite signal due to the coupling with ¹⁹⁵Pt, J_{Pt-P} = 3216 Hz). Anal. Calcd. for C₃₇H₄₅Cl₂N₂P₂O₃F₃STiPt: C, 43.12; H, 4.40; N, 2.72. Found: C, 43.48; H, 4.68; N, 3.01 %. Exact mass (ESI-TOF): Calcd. for ¹²C₃₆¹H₄₅¹⁴N₂³¹P₂³⁵Cl₂⁴⁸Ti₁¹⁹⁵Pt₁: 880.15622. Found: 880.15738.

Preparation of [(dppp)M₂(η³-methallyl)](OTf) (M = Ni (3a**), Pd (**3b**), Pt (**3c**)).**

The complexes **3a** – **3c** were prepared according to the method reported in the literature ⁵⁾ with slight modification. In a typical example, $[(\eta^3\text{-methallyl})\text{NiCl}]_2$ (29 mg, 0.10 mmol) and acetone (140 μL , 2.0 mmol) was mixed in CH_2Cl_2 (5 mL), and AgOTf (50 mg, 0.20 mmol) was added to this solution. The mixture was stirred at room temperature for 10 min, and then dppp (80 mg, 0.20 mmol) was added to this solution. The resulting mixture was stirred at room temperature for 30 min, then the solvent was evaporated, and the residue extracted with CH_2Cl_2 . The insoluble materials were filtered off through a pad of Celite, and the resulting filtrate was collected. Removal of volatiles followed by washing with hexane gave desired complex (**3a**) as white powder (102 mg, 74 %). ^1H NMR (CD_2Cl_2 , r.t.) δ 1.89 (s, 3H, CH_3), 2.50 – 2.91 (m, 6H, CH_2), 2.72 (br s, 2H, $\text{CH}_2=\text{C}(\text{CH}_3)$), 3.43 (br s, 2H, $\text{CH}_2=\text{C}(\text{CH}_3)$) 7.17 – 7.69 (m, 20H, Ph). ^{31}P $\{^1\text{H}\}$ NMR (CD_2Cl_2 , r.t.) δ -6.1 (s).

Using similar procedures, **3b** and **3c** were synthesized. **3b**: ^1H NMR (CD_2Cl_2 , r.t.) δ 1.88 (s, 3H, CH_3), 1.91 – 2.18 (m, 2H, CH_2), 2.62 – 2.81 (m, 4H, CH_2), 3.12 (t, $J_{\text{P-H}} = 6.9$ Hz, 2H, $\text{CH}_2=\text{C}(\text{CH}_3)$), 3.82 (br s, 2H, $\text{CH}_2=\text{C}(\text{CH}_3)$) 7.26 – 7.55 (m, 20H, Ph). ^{13}C NMR (CD_2Cl_2 , r.t.) δ 19.2 (s, CH_3), 24.1 (s, $-\text{CH}_2-$), 24.3 (t, $J_{\text{P-C}} = 15.9$ Hz, P- CH_2), 73.4 (t, $J_{\text{P-C}} = 15.9$ Hz, $\text{CH}_2=\text{C}(\text{CH}_3)$), 129.5 (t, $J_{\text{P-C}} = 5.8$ Hz, *meta*-Ph), 131.6 (d, $J_{\text{P-C}} = 24.5$ Hz, *para*-Ph), 132.0 (t, $J_{\text{P-C}} = 21.7$ Hz, *ipso*-Ph), 132.7 (dt, $J_{\text{P-C}} = 5.8$, 44.8 Hz, *ortho*-Ph), 138.2 (t, $J_{\text{P-C}} = 5.8$ Hz, $\text{CH}_2=\text{C}(\text{CH}_3)$). ^{31}P $\{^1\text{H}\}$ NMR (CD_2Cl_2 , r.t.) δ 8.70 (s). **3c**: ^1H NMR (CD_2Cl_2 , r.t.) δ 1.92 (s with a satellite signal due to the coupling with ^{195}Pt , $J_{\text{Pt-H}} = 59.8$ Hz, 3H, CH_3), 1.98 – 2.27 (m, 2H, CH_2), 2.58 – 2.95 (m, 4H, CH_2 , and 2H, $\text{CH}_2=\text{C}(\text{CH}_3)$), 3.55 (br s, 2H, $\text{CH}_2=\text{C}(\text{CH}_3)$) 7.24 – 7.58 (m, 20H, Ph). ^{31}P $\{^1\text{H}\}$ NMR (CD_2Cl_2 , r.t.) δ 0.25 (s with a satellite signal due to the coupling with ^{195}Pt , $J_{\text{Pt-P}} = 3512$ Hz).

Reaction of Ti-M₂ dinuclear complexes with amines. A mixture of the Ti-M₂ dinuclear complex [for **2a** (9 mg, 0.01 mmol), for **2b** (9 mg, 0.01 mmol), for **2c** (10 mg, 0.01 mmol)] and CD_2Cl_2 (0.3 mL) was transferred into a flame dried NMR tube in a glove box. A solution of amine [for HNet₂ (10 μL , 0.1 mmol), for aniline (9.2 μL , 0.1 mmol)] in CD_2Cl_2 (0.2 mL) was added to this solution, and the solution

was quickly frozen, and connected to a vacuum line. The tube was evacuated at -78 °C, sealed by flame, quickly warmed, and shaken several times. The NMR measurement was carried out periodically at 25 °C in CD₂Cl₂.

The reaction of dppp complexes (**3a**, **3b**, **3c**) with HNEt₂ or aniline were performed using similar method.

Catalytic allylation of diethylamine catalyzed by 2b. Methallyl chloride (9.4 µl, 0.1 mmol) and diethylamine (20 µl, 0.2 mmol) was dissolved in CD₂Cl₂, and 10 mol % of **2b** (9 mg, 0.01 mmol) was added to this solution. This reaction mixture was quickly transferred into a flame dried NMR tube in a glove box, and the mixture was quickly frozen. The tube was evacuated at lower temperature, sealed by flame, quickly warmed, and shaken for 5 min. Complete conversion of methallyl chloride was confirmed by the NMR measurement at 25 °C.

The reaction of dppp complexes (**3a**, **3b**, **3c**) with HNEt₂ or aniline were performed using similar method.

X-ray data collection and reduction. X-ray crystallography was performed on a Rigaku Saturn CCD area detector with graphite monochromated Mo-K α radiation ($\lambda = 0.71070\text{\AA}$). The data were collected at 123(2) K using ω scan in the θ range of $3.0 \leq \theta \leq 27.5$ deg (**2a**), $3.1 \leq \theta \leq 27.5$ deg (**2b**), $3.0 \leq \theta \leq 27.5$ deg (**2c**). The data obtained were processed using Crystal-Clear (Rigaku) on a Pentium computer, and were corrected for Lorentz and polarization effects. The structure was solved by direct methods⁶ for **2a**, **2b**, and **2c**, and expanded using Fourier techniques.⁷ The non-hydrogen atoms were refined anisotropically except for the solvent atoms (toluene for **2a** and **2c**, and CH₂Cl₂ for **2b**). Hydrogen atoms were refined using the riding model. In complex **2c**, there is a large void in the unit cell, however, it was difficult to find the solvated molecule inside the void due to the low quality of the crystal. The final cycle of full-matrix least-squares refinement on F^2 was based on 8,528 observed reflections and 601 variable parameters for **2a**, 9,835 observed reflections and 530 variable parameters for **2b**, 10,987

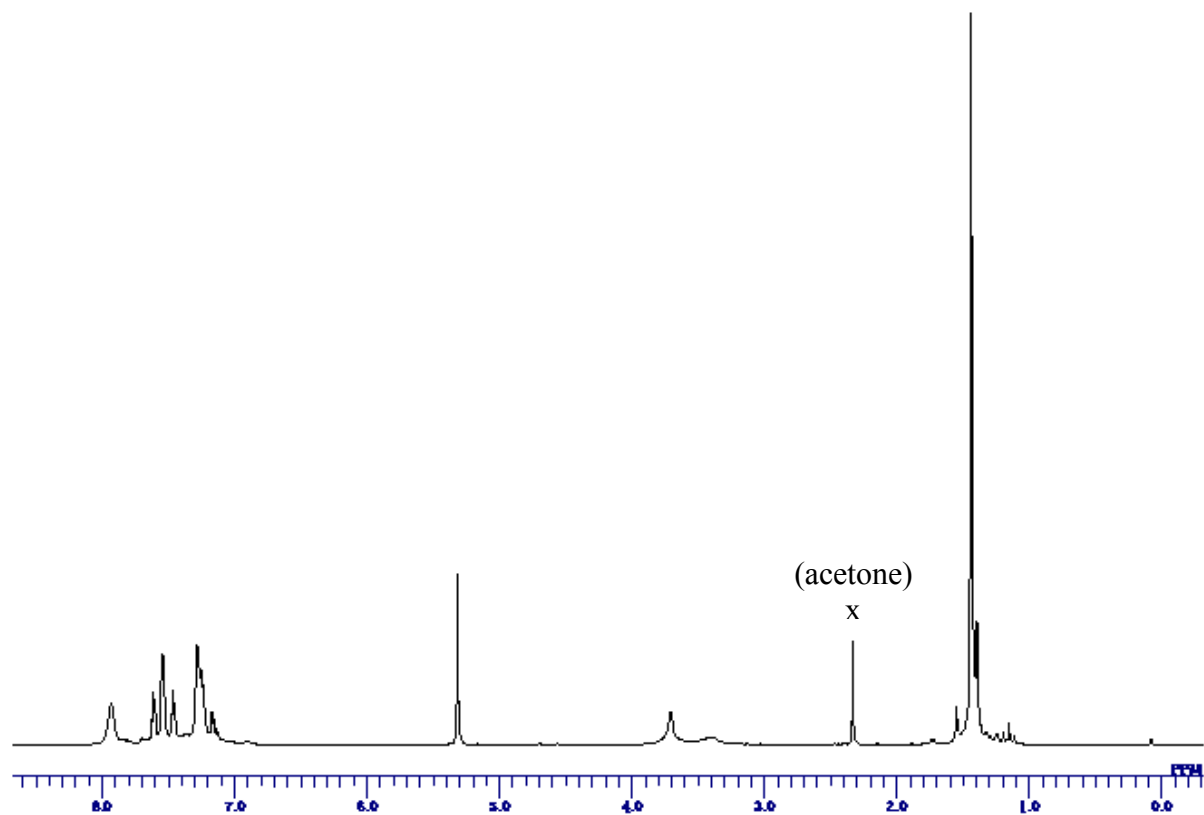
observed reflections and 521 variable parameters for **2c**. Neutral atom scattering factors were taken from Cromer and Waber.⁸ All calculations were performed using the CrystalStructure^{9,10} crystallographic software package. Details of final refinement as well as the bond distances and angles are summarized in the supporting information, and the numbering scheme employed is also shown in the supporting information, which were drawn with ORTEP at 50% probability ellipsoid.

References

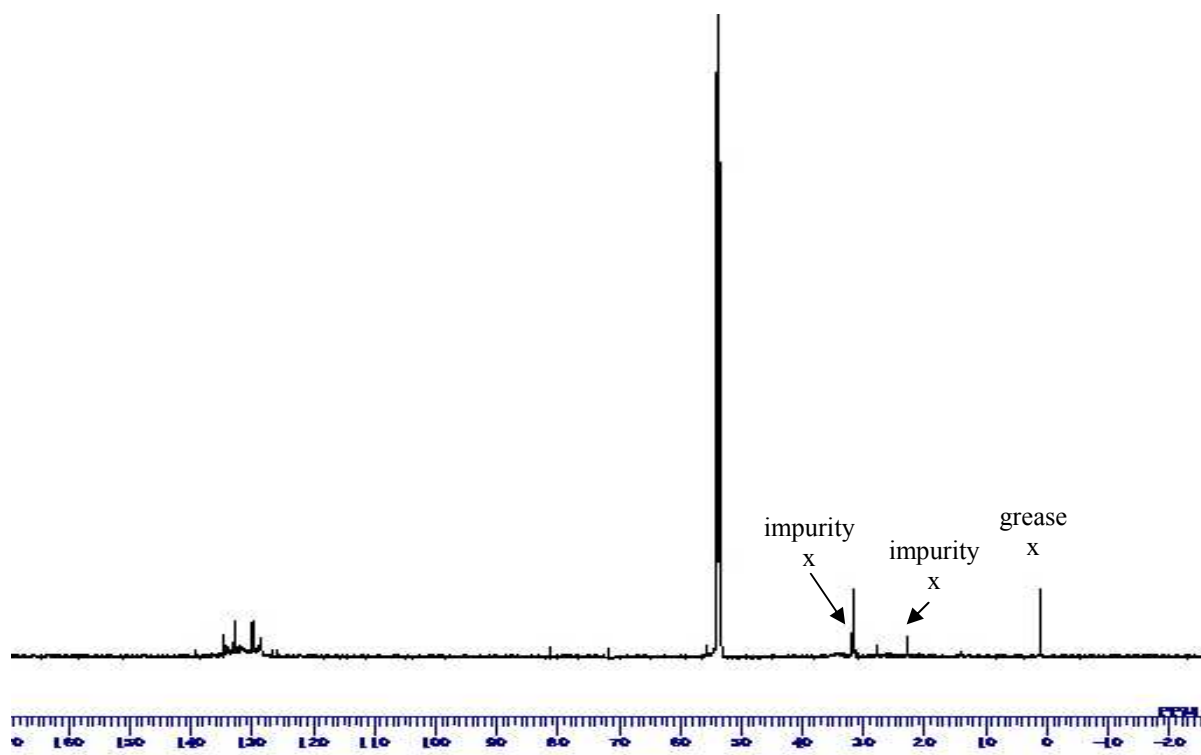
1. Nagashima, H.; Sue, T.; Oda, T.; Kanemitsu, A.; Matsumoto, T.; Motoyama, Y.; Sunada, Y. *Organometallics* **2006**, *25*, 1987
2. (a) Shim, C. B.; Kim, Y. H.; Lee, B. Y.; Dong, Y.; Yun, H. *Organometallics* **2003**, *22*, 4272. (b) Semmelhack, M. F. In *Organic Reactions*, John Wiley, **1972**, *19*, 115
3. Hartley, F. R.; Jones, S. R. *J. Organomet. Chem.*, **1974**, *66*, 465.
4. Mabbott, D. J.; Mann, B. E.; Maitlis, P. M. *J. Chem. Soc. Dalton Trans.*, **1977**, 294.
5. Thoumazet, C.; Grützmacher, H.; Deschamps, B.; Ricard, L.; le Floch, P. *Eur. J. Inorg. Chem.*, **2006**, 3911.
6. (a) SHELX97: Sheldrick, G.M. **1997**. (b) SIR97: Altomare, A.; Burla, M. C.; Camalli, M.; Cascarano, G.; Guagliardi, A.; Moliterni, A.; Polidori, G.; Spagna, R. **1999**.
7. DIRDIF99: Beurskens, P. T.; Admiraal, G.; Beurskens, G.; Bosman, W. P.; de Gelder, R.; Israel, R.; Smits, J. M. M. The DIRDIF-99 program system; *Technical Report of the Crystallography Laboratory*; University of Nijmegen, Nijmegen, The Netherlands, **1999**.
8. Cromer, D. T.; Waber, J. T. *International Tables for X-ray Crystallography*; Kynoch Press: Birmingham, U.K., **1974** Vol. 4.

9. CrystalStructure 3.8.0: Crystal Structure Analysis Package; Package, Rigaku and Rigaku/MSC. 9009 New Trails Dr. The Woodlands TX 77381 USA. **2000-2006**.
10. CRYSTALS Issue 11: Carruthers, J.R.; Rollett, J.S.; Betteridge, P.W.; Kinna, D.; Pearce, L.; Larsen, A.; Gabe, E. *Chemical Crystallography Laboratory*; Oxford, U.K., **1999**.

Figure S1. ^1H , ^{13}C , ^{19}F , and ^{31}P NMR spectra of $[(\eta^3\text{-methallyl})\text{Ni}(\text{Ph}_2\text{PN}^t\text{Bu})_2\text{TiCl}_2](\text{OTf})$ (**2a**)

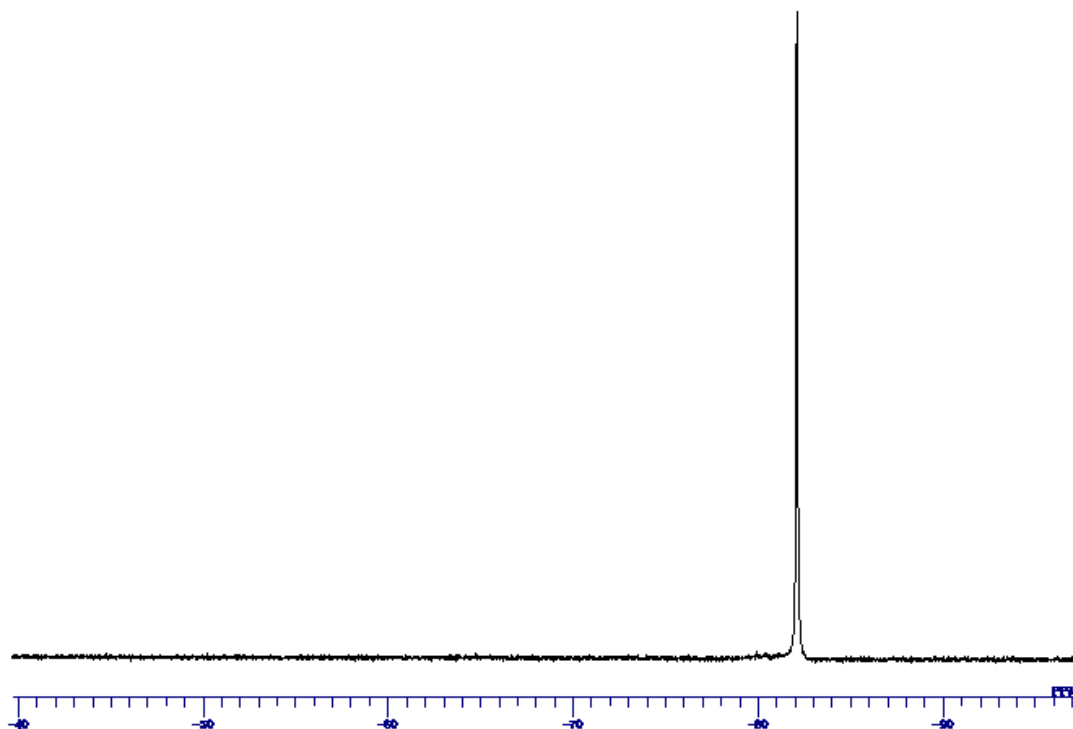


^1H NMR (600 MHz, in CD_2Cl_2)

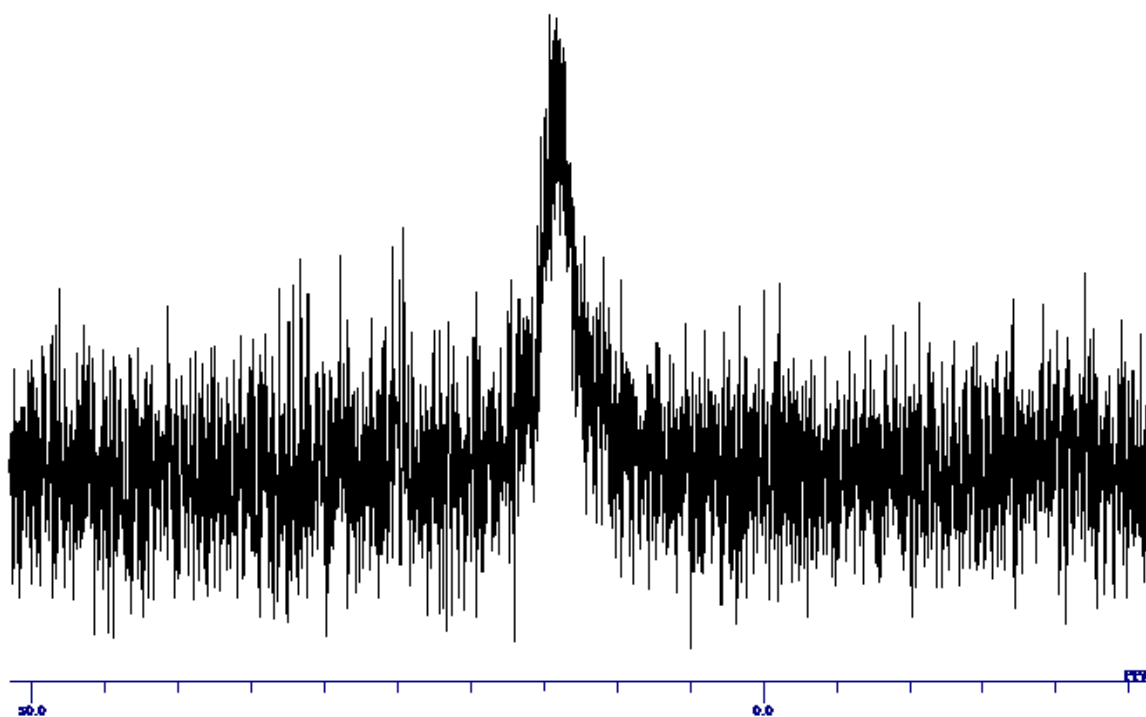


^{13}C NMR (150 MHz, in CD_2Cl_2)

Figure S1. ^1H , ^{13}C , ^{19}F , and ^{31}P NMR spectra of $[(\eta^3\text{-methallyl})\text{Ni}(\text{Ph}_2\text{PN}^t\text{Bu})_2\text{TiCl}_2](\text{OTf})$ (**2a**) (continued)

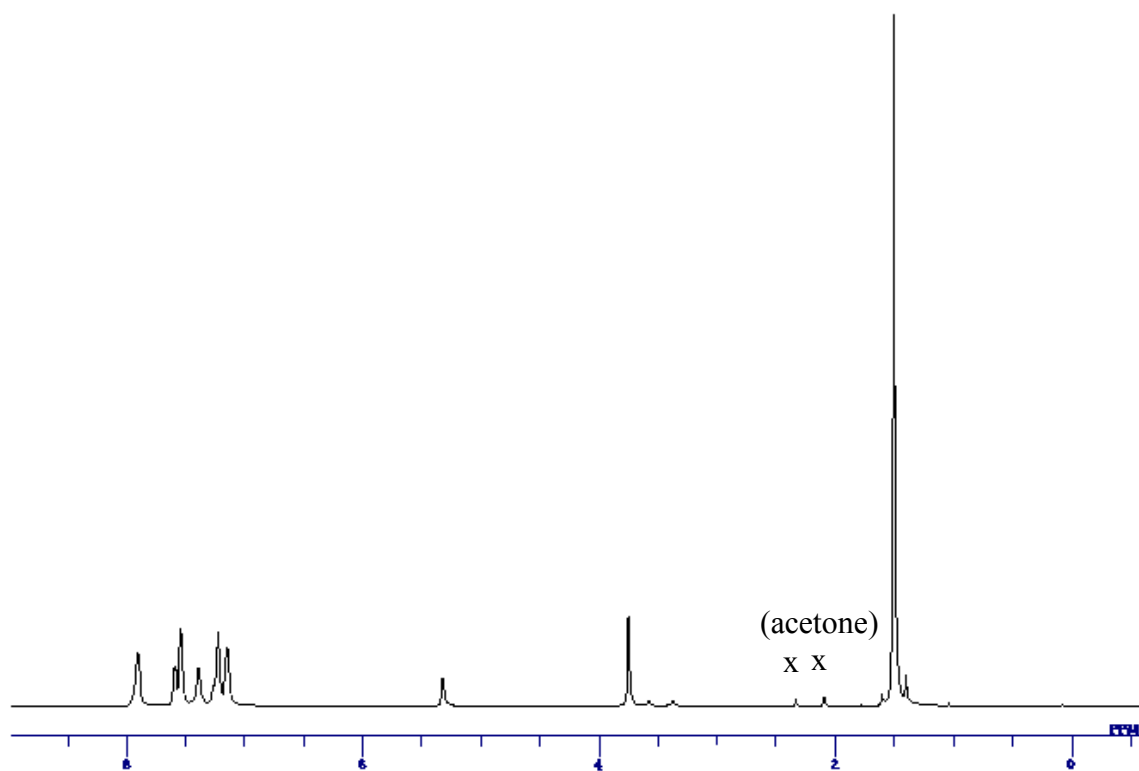


^{19}F NMR (565 MHz, in CD_2Cl_2)

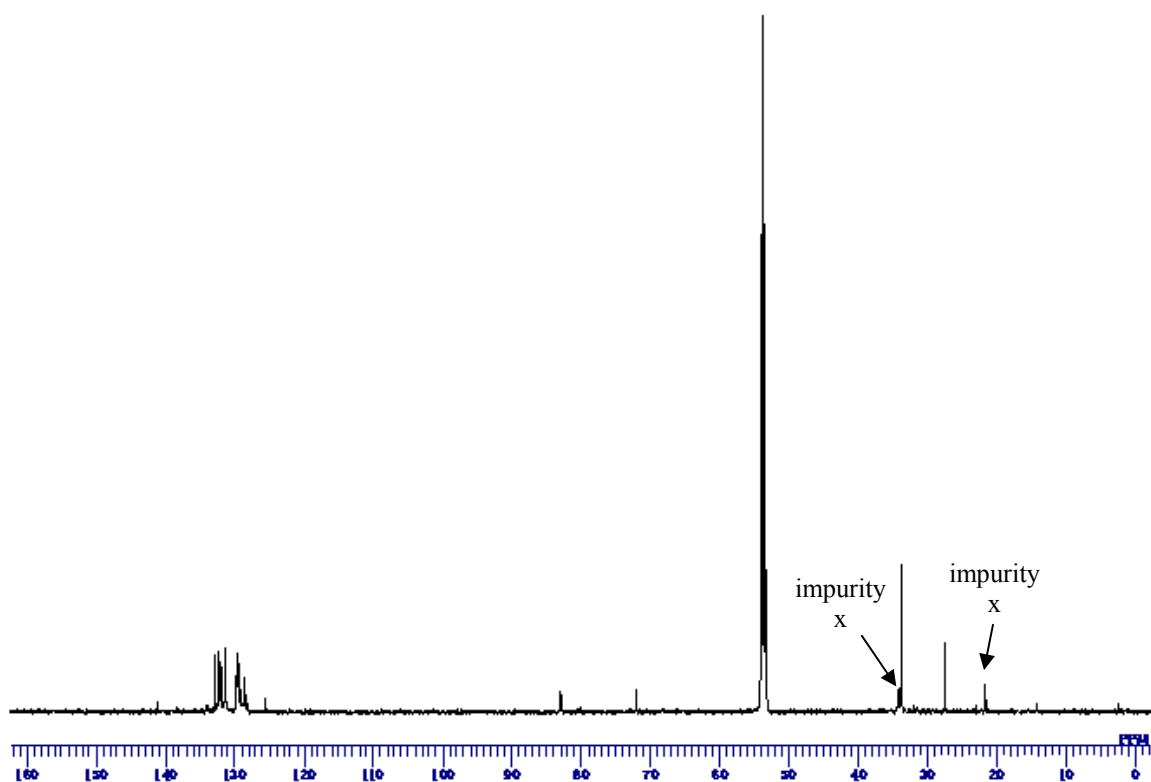


^{31}P NMR (243 MHz, in CD_2Cl_2)

Figure S2. ^1H , ^{13}C , ^{19}F , and ^{31}P NMR spectra of $[(\eta^3\text{-methallyl})\text{Pd}(\text{Ph}_2\text{PN}^t\text{Bu})_2\text{TiCl}_2](\text{OTf})$ (**2b**)

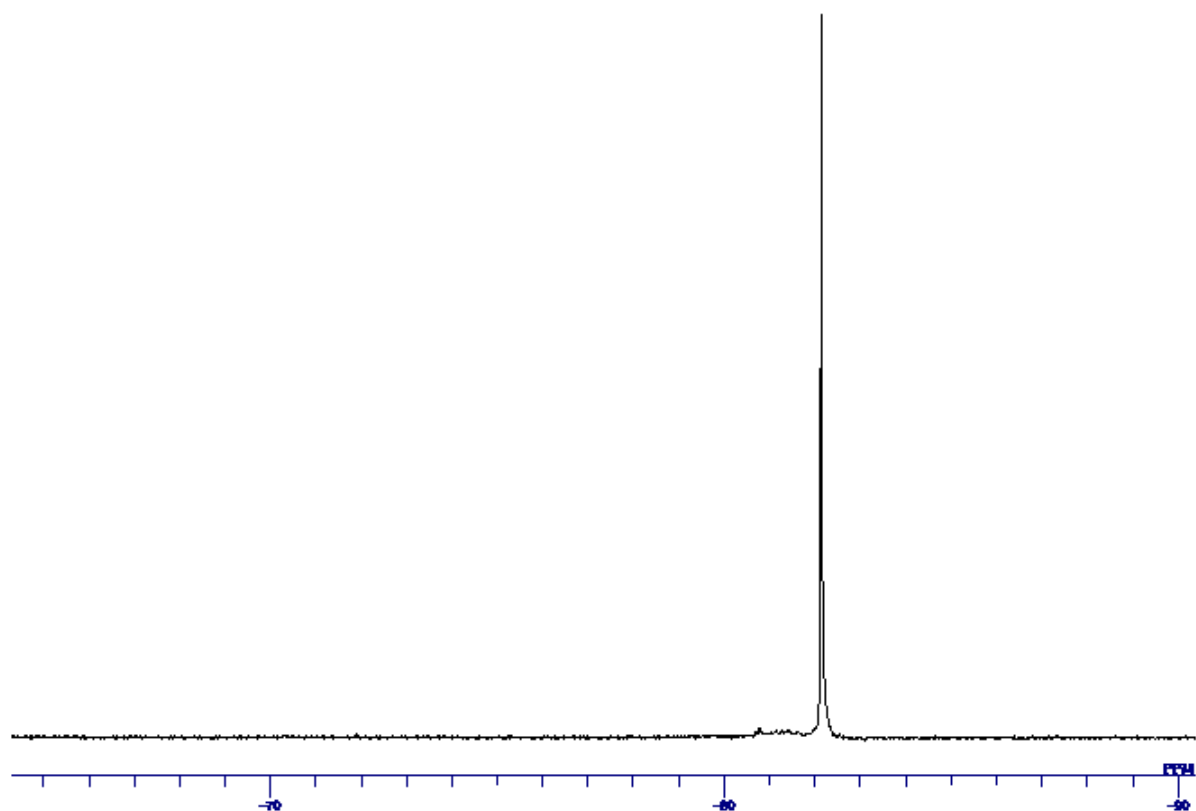


^1H NMR (600 MHz, in CD_2Cl_2)

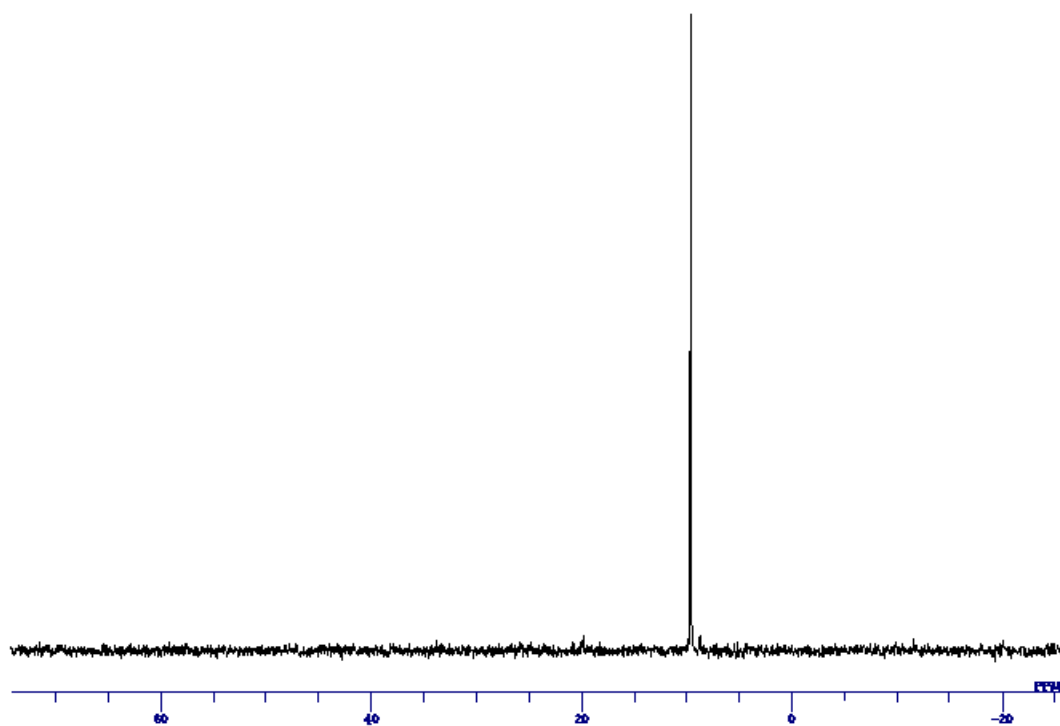


^{13}C NMR (150 MHz, in CD_2Cl_2)

Figure S2. ^1H , ^{13}C , ^{19}F , and ^{31}P NMR spectra of $[(\eta^3\text{-methallyl})\text{Pd}(\text{Ph}_2\text{PN}^t\text{Bu})_2\text{TiCl}_2](\text{OTf})$ (**2b**) (continued)

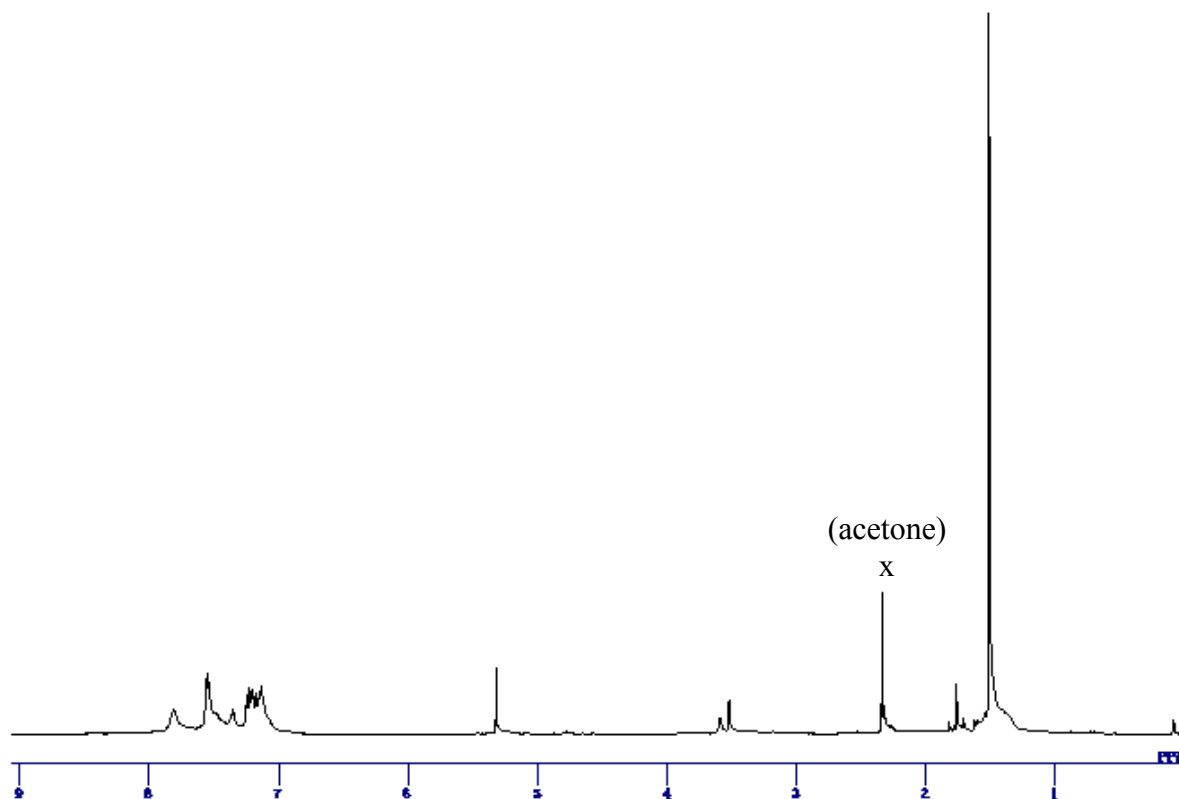


^{19}F NMR (565 MHz, in CD_2Cl_2)

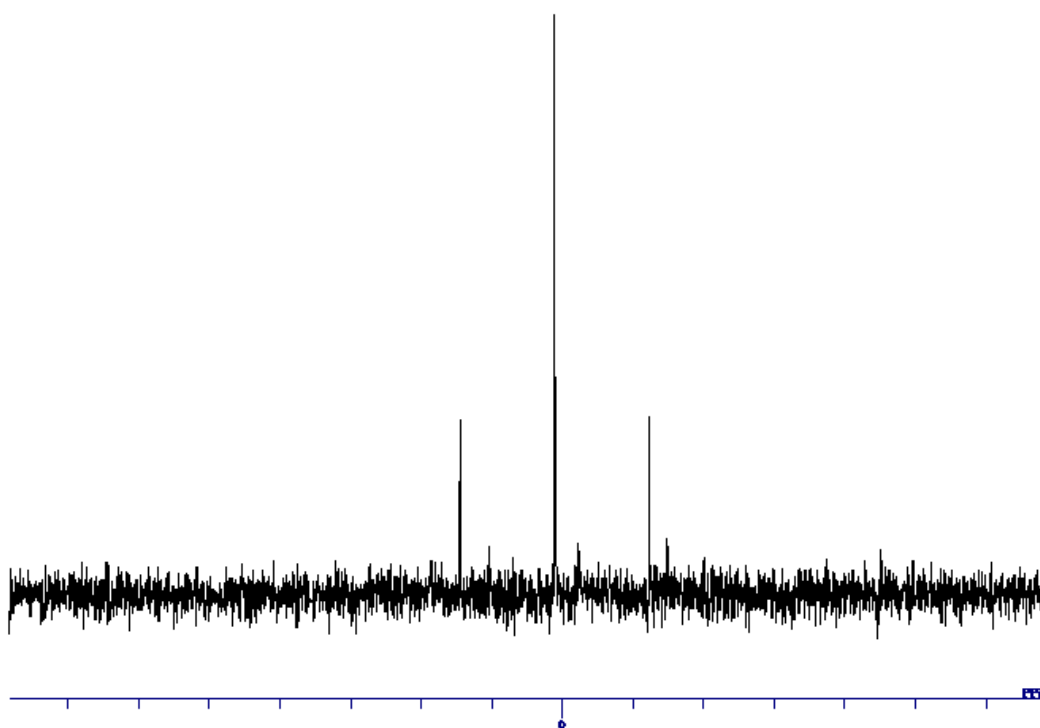


^{31}P NMR (243 MHz, in CD_2Cl_2)

Figure S3. ^1H , ^{13}C , ^{19}F , and ^{31}P NMR spectra of $[(\eta^3\text{-methallyl})\text{Pt}(\text{Ph}_2\text{PN}^t\text{Bu})_2\text{TiCl}_2](\text{OTf})$ (**2c**)



^1H NMR (600 MHz, in CD_2Cl_2)



^{31}P NMR (243 MHz, in CD_2Cl_2)

Figure S4. VT- ^1H and ^{31}P NMR spectra of $[(\eta^3\text{-methallyl})\text{Ni}(\text{Ph}_2\text{PN}^t\text{Bu})_2\text{TiCl}_2](\text{OTf})$ (**2a**)

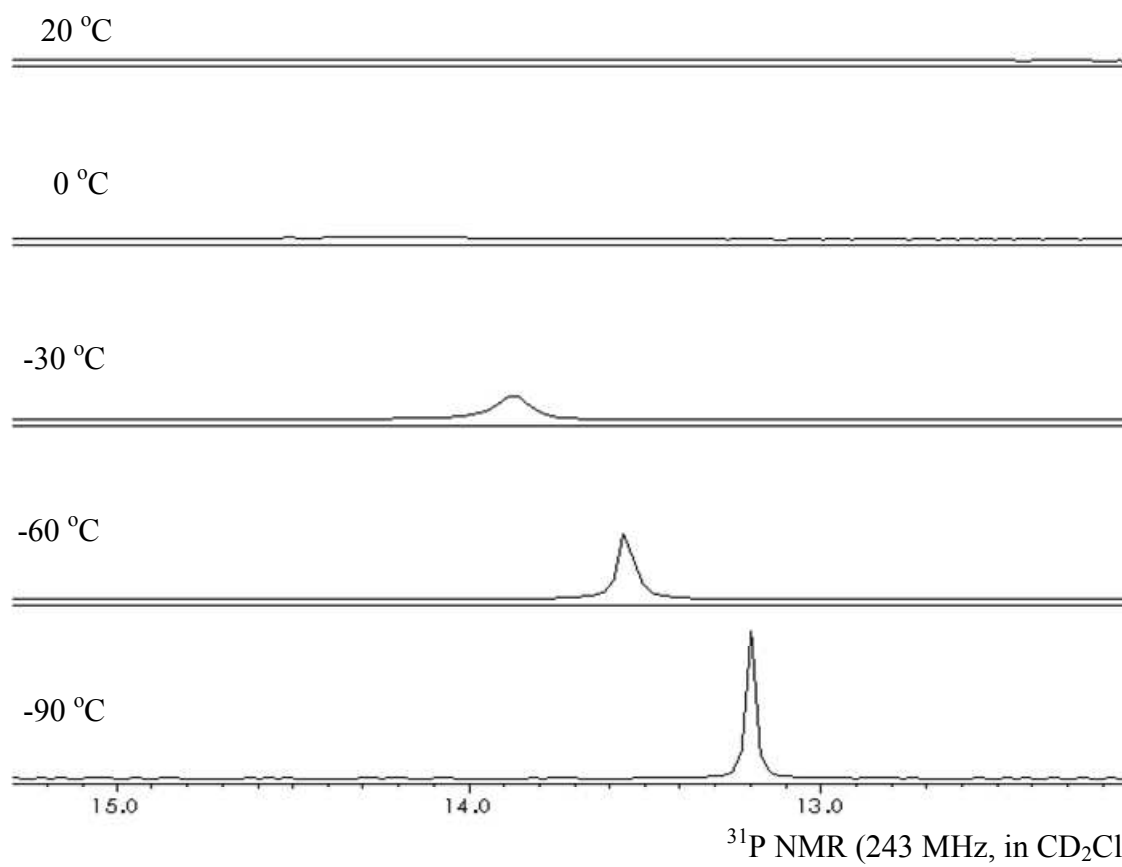
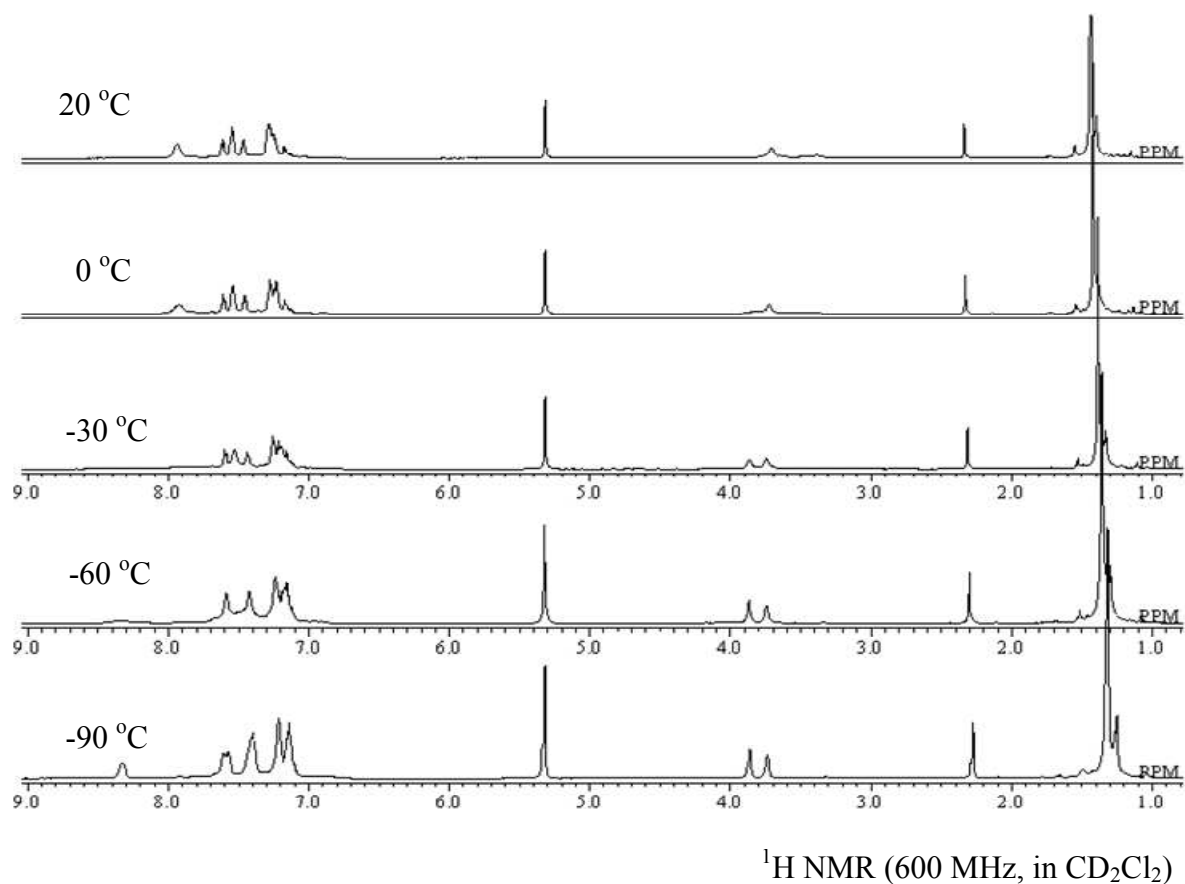


Figure S5. VT- ^1H and ^{31}P NMR spectra of $[(\eta^3\text{-methallyl})\text{Pd}(\text{Ph}_2\text{PN}^t\text{Bu})_2\text{TiCl}_2](\text{OTf})$ (**2b**)

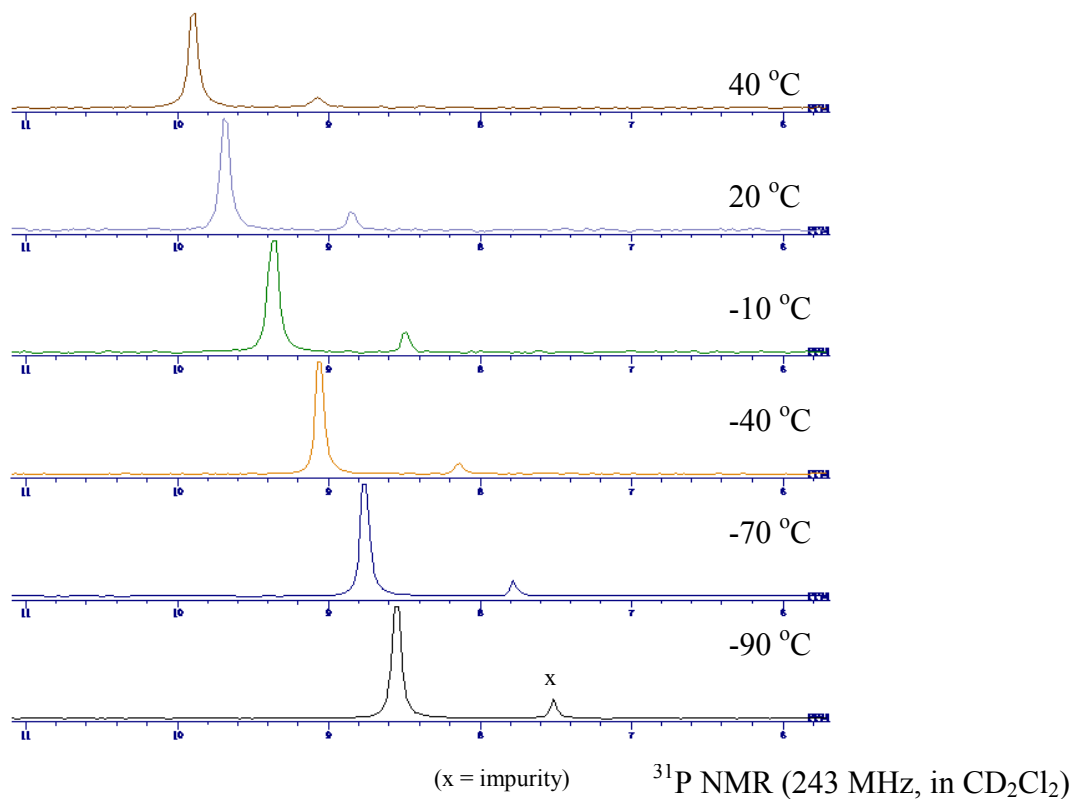
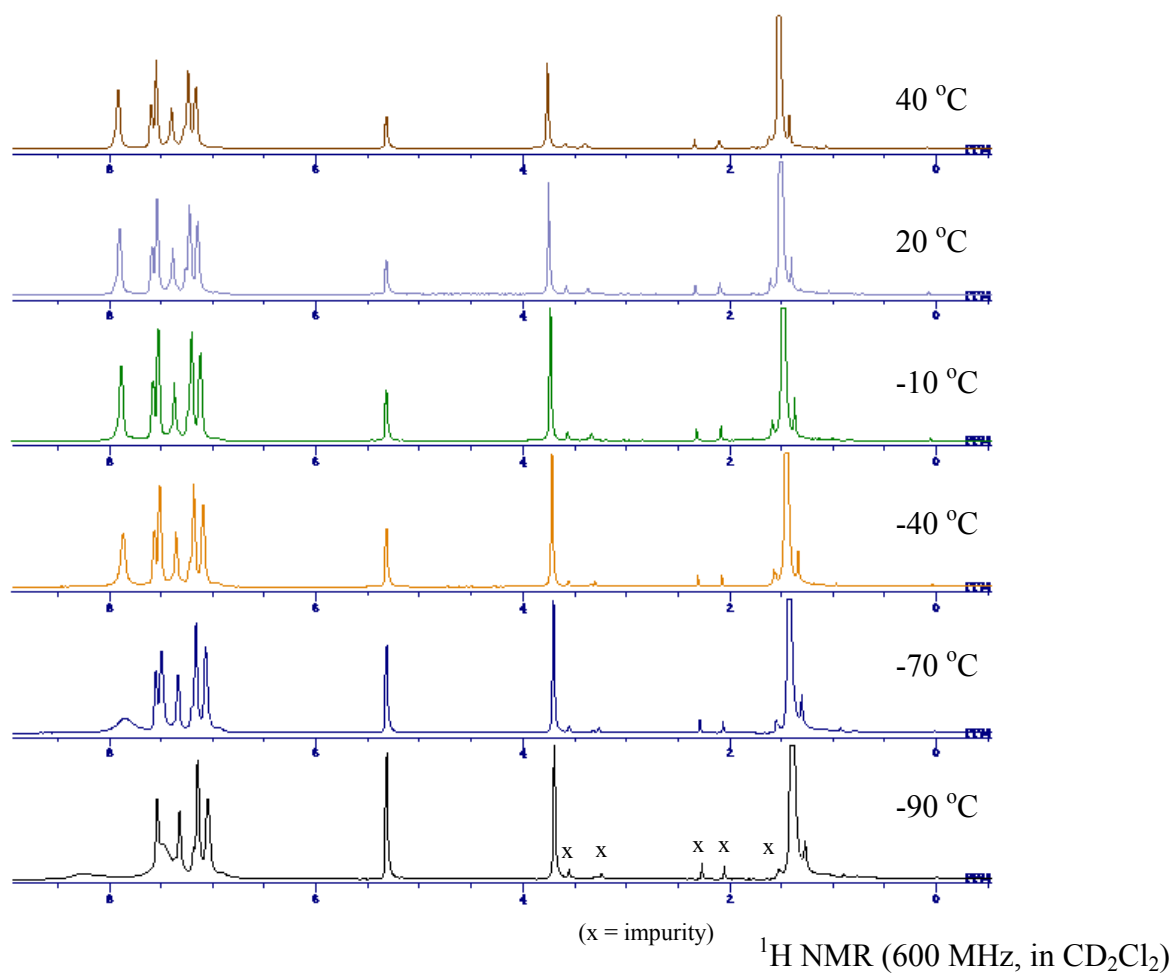
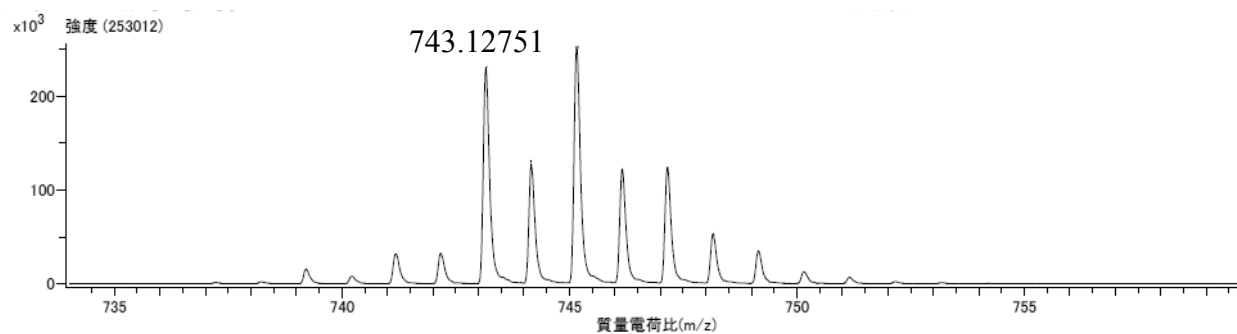


Figure S6. ESI-(tof)-MS spectrum of $[(\eta^3\text{-methallyl})\text{Ni}(\text{Ph}_2\text{PN}^t\text{Bu})_2\text{TiCl}_2](\text{OTf})$ (**2a**)

Actual spectrum



Simulated

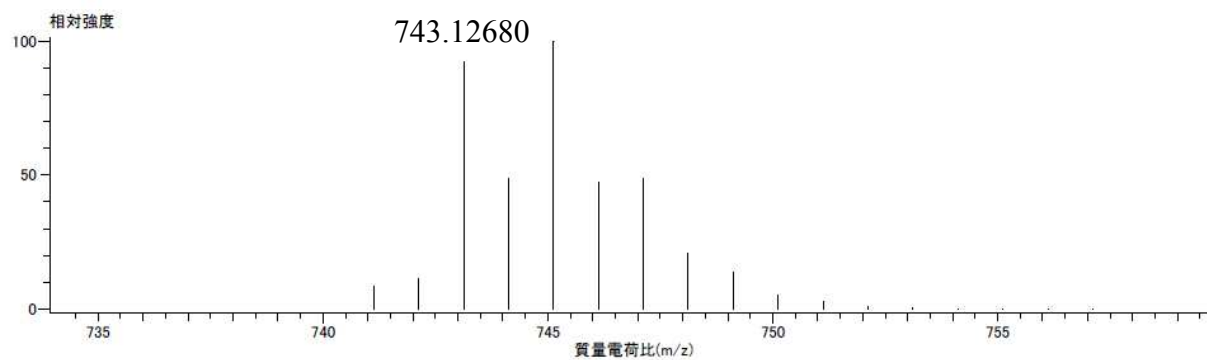
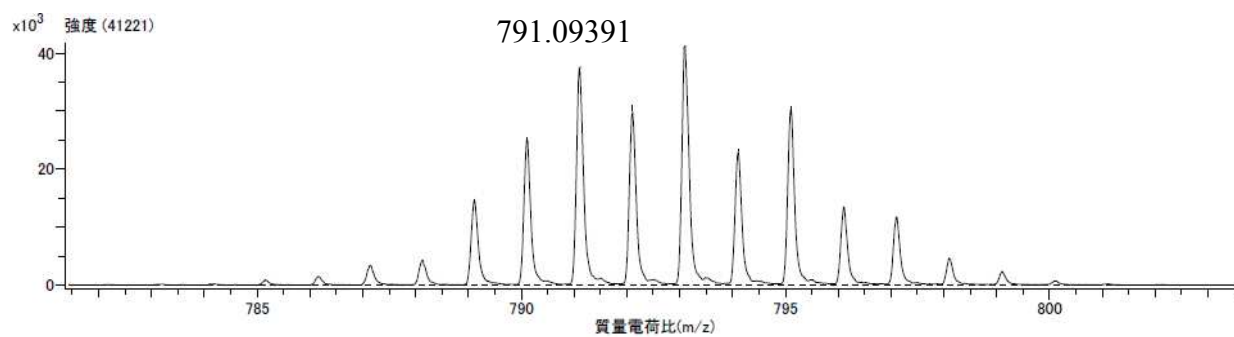


Figure S7. ESI-(tof)-MS spectrum of $[(\eta^3\text{-methallyl})\text{Pd}(\text{Ph}_2\text{PN}^t\text{Bu})_2\text{TiCl}_2](\text{OTf})$ (**2b**)

Actual spectrum



Simulated

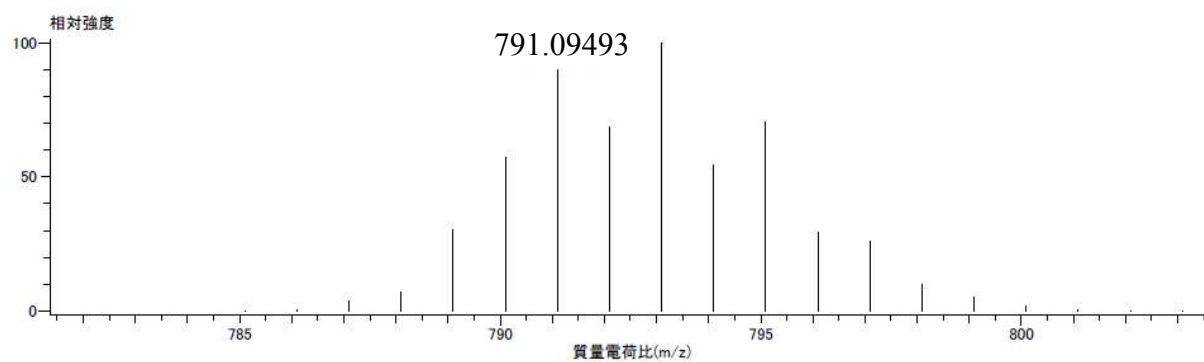
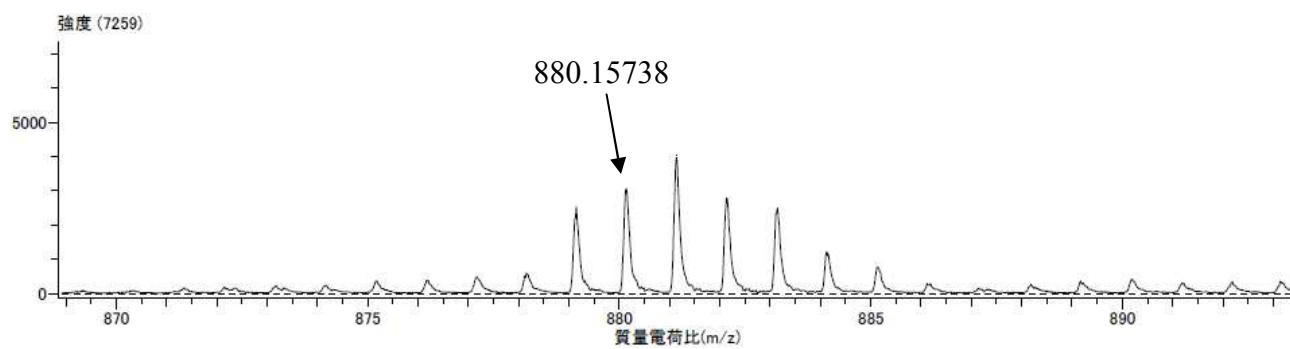


Figure S8. ESI-(tof)-MS spectrum of $[(\eta^3\text{-methallyl})\text{Pt}(\text{Ph}_2\text{PN}^t\text{Bu})_2\text{TiCl}_2](\text{OTf})$ (**2c**)

Actual spectrum



Simulated

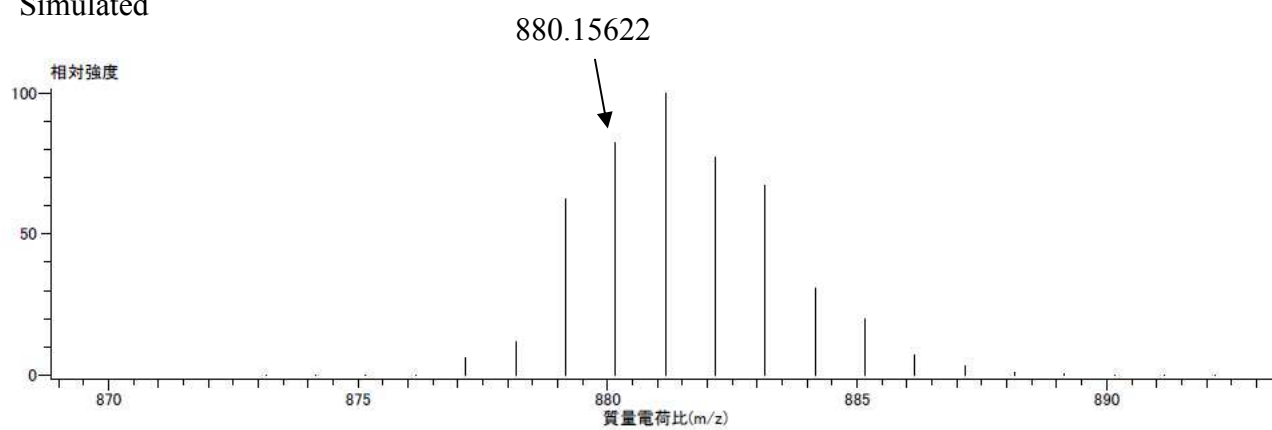


Table S1. Crystallographic data for **2a**, **2b**, and **2c**.

	2a	2b	2c
Empirical Formula	C ₃₇ H ₄₅ Cl ₂ F ₃ N ₂ NiO ₃ P ₂ STi·1.5C ₇ H ₈	C ₃₇ H ₄₅ Cl ₂ F ₃ N ₂ O ₃ P ₂ Pd STi·0.5 CH ₂ Cl ₂	C ₃₇ H ₄₅ Cl ₂ F ₃ N ₂ O ₃ P ₂ PtS Ti·0.5 C ₇ H ₈
Formula Weight	1010.47	992.65	1076.74
Crystal System	monoclinic	monoclinic	monoclinic
Lattice Type	Primitive	Primitive	Primitive
Space Group	P2 ₁ /c (#14)	P2 ₁ /n (#14)	P2 ₁ /c (#14)
a, Å	20.222(7)	11.1976(13)	19.813(3)
b, Å	15.556(5)	18.604(2)	15.645(2)
c, Å	15.826(5)	21.654(2)	15.723(2)
α, deg.	90	90	90
β, deg.	102.066(6)	101.6701(17)	99.555(2)
γ, deg.	90	90	90
Volume, Å ³	4869(3)	4417.6(8)	4806.2(12)
Z value	4	4	4
D _{calc} , g/cm ³	1.378	1.492	1.488
F(000)	2102.00	1952.00	2148.00
μ(MoKα), cm ⁻¹	8.207	9.978	33.302
Crystal Color, Habit	Dark red, block	Red, block	red, platelet
Crystal Dimensions, mm	0.18 x 0.16 x 0.05	0.25 x 0.20 x 0.10	0.10 x 0.05 x 0.03
No. Observations (All reflections)	8528	9835	10987
No. Variables	601	530	521
Reflection/Parameter Ratio	14.19	18.56	21.09
R (All reflections)	0.1460	0.0617	0.0652
R ₁ (I>2.00σ(I)) ^a	0.0961	0.0552	0.0866
wR ₂ (All reflections) ^b	0.2857	0.1946	0.2077
GOF	1.000	1.003	1.002
Max Shift/Error in Final Cycle	0.000	0.000	0.000
Maximum peak in Final Diff. Map, e ⁻ /Å ³	3.46	4.37	5.92
Minimum peak in Final Diff. Map, e ⁻ /Å ³	-0.95	-2.03	-3.11

^{a)} $R_1 = \sum |F_o| - |F_c| / \sum |F_o|$ ^{b)} $wR_2 = [\sum (w(F_o^2 - F_c^2)^2) / \sum (w(F_o^2)^2)]^{1/2}$

Table S2. Representative bond lengths and angles for **2a**, **2b**, and **2c**.

	2a	2b	2c
	bond length (Å)		
M-Ti	2.6036(18)	2.8155(5)	2.7653(15)
M-Cl(1)	2.692(2)	3.0291(9)	3.124(2)
M-C(1)	2.082(8)	2.222(3)	2.179(10)
M-C(2)	2.093(9)	2.245(3)	2.247(10)
M-C(3)	2.041(10)	2.171(3)	2.205(9)
M-P(1)	2.240(2)	2.3244(9)	2.2889(17)
M-P(2)	2.237(2)	2.3061(9)	2.2903(17)
Ti-Cl(1)	2.313(2)	2.2958(11)	2.286(2)
Ti-Cl(2)	2.246(2)	2.2337(9)	2.229(3)
Ti-N(1)	1.942(6)	1.939(3)	1.951(5)
Ti-N(2)	1.945(5)	1.946(2)	1.957(5)
Ti-P(1)	2.689(2)	2.7495(10)	2.780(2)
Ti-P(2)	2.699(2)	2.7534(10)	2.764(2)
N(1)-P(1)	1.656(7)	1.676(2)	1.658(6)
N(2)-P(2)	1.657(7)	1.664(2)	1.635(6)
	bond angle (deg.)		
P(1)-M-P(2)	111.33(8)	107.37(3)	108.17(6)
C(1)-M-C(2)	39.4(3)	36.71(13)	36.1(4)
C(1)-M-C(3)	70.1(3)	66.00(13)	65.5(3)
C(2)-M-C(3)	40.0(3)	37.49(13)	36.9(3)
P(1)-M-C(1)	88.9(2)	93.44(9)	93.1(2)
P(1)-M-C(2)	111.6(2)	121.84(9)	121.8(2)
P(1)-M-C(3)	156.5(2)	158.78(9)	158.1(2)
P(2)-M-C(1)	156.1(2)	156.50(9)	156.5(2)
P(2)-M-C(2)	117.0(2)	119.99(9)	120.6(2)
P(2)-M-C(3)	87.3(2)	92.02(9)	92.3(2)
N(1)-Ti-N(2)	116.4(2)	116.38(12)	116.2(2)
N(1)-Ti-Cl(1)	117.35(19)	114.56(9)	117.99(19)
N(1)-Ti-Cl(2)	102.8(2)	102.71(8)	102.5(2)
N(2)-Ti-Cl(1)	117.5(2)	121.56(8)	119.29(19)
N(2)-Ti-Cl(2)	103.9(2)	100.78(8)	101.7(2)
Cl(1)-Ti-Cl(2)	93.05(9)	94.15(3)	91.53(11)

A 3D molecular model of the NiTi complex. The structure features a central metal core with a titanium (Ti) atom (blue sphere) and a nickel (Ni) atom (orange sphere). The surrounding ligands are represented by white spheres (hydrogen) and red/green spheres (oxygen/nitrogen). The electron density is visualized using green and red isosurfaces, with a label 'Ti' pointing to the blue sphere and 'Ni' pointing to the orange sphere.

Figure S11. ORTEP representation of the molecular structure of $[(\eta^3\text{-methallyl})\text{Pd}(\text{Ph}_2\text{PN}^t\text{Bu})_2\text{TiCl}_2](\text{OTf})$ (**2b**) showing 50 % probability ellipsoids. Counter anion, solvent molecule (CH_2Cl_2), and hydrogen atoms were omitted for clarity.

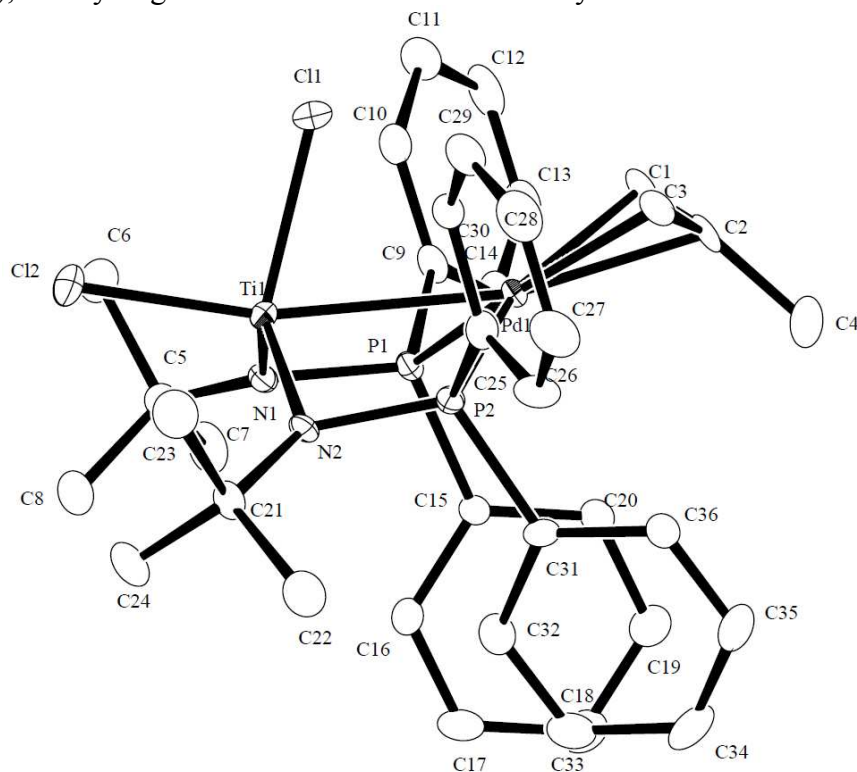


Figure S12. Gaussview depiction of HOMO-1 for the calculated complex $[(\eta^3\text{-methallyl})\text{Pd}(\text{Ph}_2\text{PN}^t\text{Bu})_2\text{TiCl}_2](\text{OTf})$ (**2b**)

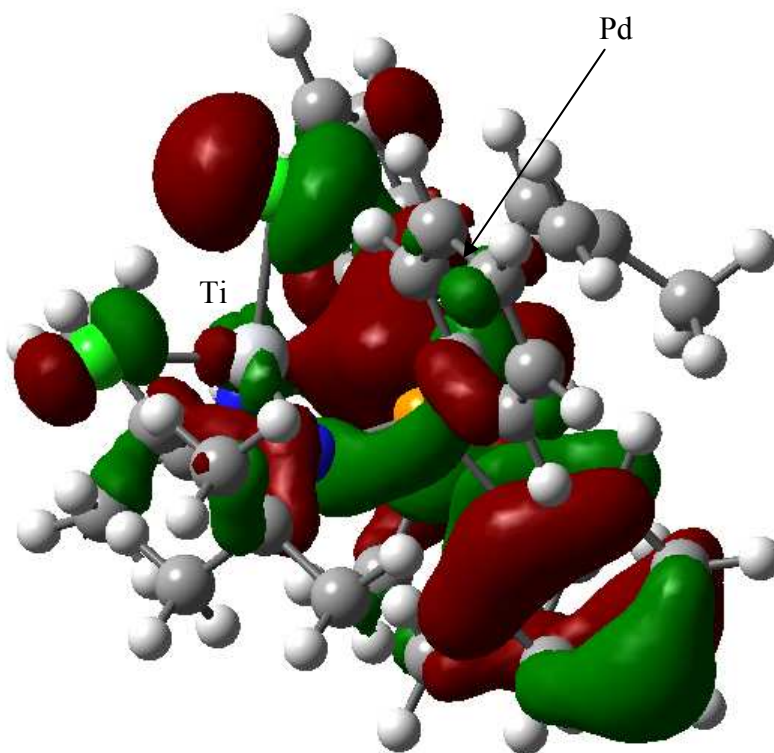


Figure S13. ORTEP representation of the molecular structure of $[(\eta^3\text{-methallyl})\text{Pt}(\text{Ph}_2\text{PN}^t\text{Bu})_2\text{TiCl}_2](\text{OTf})$ (**2c**) showing 50 % probability ellipsoids. Hydrogen atoms were omitted for clarity. Counter anion, solvent molecule (toluene), and hydrogen atoms were omitted for clarity.

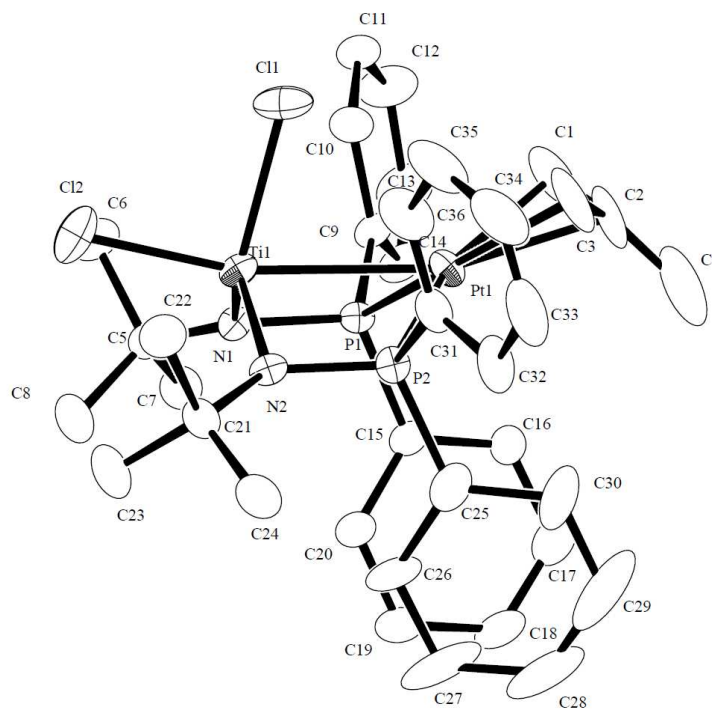


Figure S14. Gaussview depiction of HOMO for the calculated complex $[(\eta^3\text{-methallyl})\text{Pt}(\text{Ph}_2\text{PN}^t\text{Bu})_2\text{TiCl}_2](\text{OTf})$ (**2c**)

